Interval model updating: method and application

H. Haddad Khodaparast, J.E. Mottershead, K.J. Badcock
University of Liverpool, School of Engineering,
Harrison-Hughes Building, The Quadrangle, L69 3GH, Liverpool, United Kingdom
e-mail: **j.e.mottershead@liverpool.ac.uk**

Abstract
The problem of interval model updating in the presence of uncertain measured data is defined and solved in two cases. The parameter vertex solution is used for the first case. It is shown that the parameter vertex solution is valid for particular parameterisation of the finite element model and particular output data. The problem is solved in the second case by using a meta-model (Kriging predictor in this paper) which acts as a surrogate for the full FE model so that regions of input data are mapped to region of output data with parameters obtained by regression analysis. The method is validated numerically using a three degree of freedom mass-spring system with close modes and experimentally using multiple sets of a frame structure with different internal beams locations.

1 Introduction

Finite element techniques are nowadays essential tools in engineering design of civil and mechanical structures. The prediction of finite element model can be improved by using deterministic finite element model updating approaches [1, 2]. These techniques are about improving and correcting invalid assumptions by processing experimental results. However experimental data includes variability due to different sources. Experimental variability is supposed not to be inherent to the test structure itself, but arises from other sources such as measurement noise, the use of sensors that affect the measurement or signal processing that might introduce bias. Such variability is reducible by increased information. Statistical techniques such as minimum variance method [3, 4] have been implemented in deterministic finite element model updating to treat reducible uncertainty in measured data. However, manufacturing and material variability in structures is not reducible and needs to be considered as part of the model. The problem of interval model updating in presence of irreducible uncertain measured data (manufacturing and material variability) is considered in this paper.

Fonseca et al. [5] proposed an optimisation procedure for the purpose of stochastic model updating based on the maximising a likelihood function and applied it to a cantilever beam with a point mass at an uncertain location. Hua et al. [6] used perturbation theory in the problem of test-structure variability. The predicted output mean values and the matrix of predicted covariances were made to converge upon measured values and in so doing the first two statistical moments of the uncertain updating parameters were determined. Khodaparast et al. [7] developed two perturbation methods for stochastic model updating. The first method required only the first order sensitivity matrix and therefore was computationally efficient compared with the method developed by Hua et al. [6] which needed the calculation of the second order sensitivity matrix. Khodaparast and Mottershead [8], and also Govers and Link [9], proposed an objective function for the purpose of stochastic model updating. The objective function consisted of two parts: 1- the Euclidean norm of the difference between mean values of measured data and analytical output vectors, and 2- the Frobenius norm of the difference between the covariance matrices of measured data and analytical outputs.

The stochastic model updating methods have made use of probabilistic model for updating so far. This usually needs large volumes of data with consequent high costs. The interval model can be used as an alternative approach when that large quantities of test data are not available. In the present article the problem of interval model updating in the presence of irreducible uncertain measured data is defined. Solutions of the problem are made available in two cases. In the first case, the problem is solved by using the parameter vertex solution [10]. It is shown that the parameter vertex solution can be only used when (i) the overall mass and stiffness matrices are linear functions of the updating parameters, (ii) can be decomposed into non-negative-definite substructure mass and stiffness matrices and (iii) the output data are the eigenvalues of the dynamic system. Two recursive updating equations are developed to update the bounds of an initial hypercube of updating parameters in this case. However, the parameter vertex solution cannot be used when the output data include the eigenvectors of the structural dynamic system and the system matrices are non-linear functions of the updating parameters. In this case, the problem is solved by using a meta-model which acts as a surrogate for the full finite element model so that the region of input data is mapped to the region of output data with parameters obtained by regression analysis. The Kriging predictor is chosen as the meta-model in this paper and is shown to be capable of predicting the region of input and output parameter variations with very good accuracy, even in the difficult case of close modes. The method is validated numerically by using a three degree of freedom mass-spring system with close modes. The method is also applied to a frame structure with uncertain internal beams locations. It is shown that the updated bounds are in good agreement with the known real bounds on the position of the beams. An extended version of this paper has been submitted to the journal of Mechanical Systems and Signal Processing [11].

2 Theory

2.1 Case 1: Parameter vertex solution

In this case, the global mass and stiffness matrices may be expanded as linear functions of the updating parameters,

$$\mathbf{M} = \mathbf{M}_0 + \sum_{j=1}^{p_1} m_j \mathbf{M}_j \tag{1}$$

$$\mathbf{K} = \mathbf{K}_0 + \sum_{j=1}^{p_2} k_j \mathbf{K}_j \tag{2}$$

where $\mathbf{M}$ is the global mass matrix, $\mathbf{K}$ is the global stiffness matrix, m_j is the updating parameter for the j^{th} substructure mass matrix, $\mathbf{M}_j$, and k_j is the updating parameter for the j^{th} substructure stiffness matrix, $\mathbf{K}_j$. The decompositions in Eqs. (1) and (2) are non-negative decompositions of the mass and stiffness matrices [10] because the substructure matrices are all semi-positive definite. From the eigenvalue derivatives of the global system [12] , it can be seen that the signs of the derivatives of the eigenvalues with respect to the updating parameters do not change within their variation in $\left[\underline{\boldsymbol{\theta}} \quad \overline{\boldsymbol{\theta}}\right]$. Therefore, the eigenvalues of the dynamic system increase monotonically with the stiffness parameters and decreases monotonically with the mass parameters. Consequently, two recursive equations can be defined to update the initial hypercube of updating parameters based on the vertices of measured data as,

$$\overline{\mathbf{z}}_m = \overline{\mathbf{z}}_l + \mathbf{S}\left|_{\boldsymbol{\theta}_{l,\overline{\mathbf{z}}_m}} \left(\boldsymbol{\theta}_{l+1,\overline{\mathbf{z}}_m} - \boldsymbol{\theta}_{l,\overline{\mathbf{z}}_m}\right)\right. \tag{3}$$

$$\underline{\mathbf{z}}_m = \underline{\mathbf{z}}_l + \mathbf{S}\left|_{\boldsymbol{\theta}_{l,\underline{\mathbf{z}}_m}} \left(\boldsymbol{\theta}_{l+1,\underline{\mathbf{z}}_m} - \boldsymbol{\theta}_{l,\underline{\mathbf{z}}_m}\right)\right. \tag{4}$$

where $\overline{\bullet}$ and $\underline{\bullet}$ denote upper bounds and lower bounds respectively, $\boldsymbol{\theta}_{l,\overline{\mathbf{z}}_m} = \left[\overline{\mathbf{k}}_l \;\; \underline{\mathbf{m}}_l\right]^{\mathrm{T}}$ and $\boldsymbol{\theta}_{l,\underline{\mathbf{z}}_m} = \left[\underline{\mathbf{k}}_l \;\; \overline{\mathbf{m}}_l\right]^{\mathrm{T}}$ and $\mathbf{S}\left|_{\boldsymbol{\theta}_{l,\cdot}}\right.$ is the sensitivity matrix evaluated at $\boldsymbol{\theta}_{l,\cdot}$, l is the iteration number and $\mathbf{z}_l$ and $\mathbf{z}_m$ are vectors containing frequencies of numerical model at l^{th} iteration and measured frequencies respectively.

2.2 Case 2: General case

As mention in the previous case, the parameter vertex solution is valid when the mass and stiffness matrices are linear functions of the updating parameters and the output data are the eigenvalues of the dynamic system. However it is shown in [11] that the parameter vertex solution is not necessarily valid for the problem of interval model updating when the output data includes both eigenvalues and eigenvectors and the mass and stiffness matrices are not linear functions of the updating parameters. In this case a meta-model as a surrogate for the finite-element model may lead to a solution with very good accuracy depending on the type of meta-model, sampling used for construction of the meta-model and the behaviour of the output functions within the region of variation. Selection of the meta-model is a crucial step in that it influences the performance of the updating procedure to a very significant degree. The Kriging estimator is chosen in this paper. The details of the Kriging estimator and optimal sampling is discussed in [11, 13, 14] and in this paper we just show the formulation of the interval model updating using Kriging estimator.

2.2.1 The Kriging Predictor in Interval Model Updating

In this section, we apply the Kriging predictor to the problem of interval model updating in structural dynamics. The details of Kriging predictor is explained in [11]. The method is originally developed by Sacks et al. [13] where further details about the method can be found. A generalised form of the Kriging predictor for a dynamic system with n output data may be written as,

$$\hat{\mathbf{z}} = \boldsymbol{\alpha} + \mathbf{H}(\boldsymbol{\theta})\,\boldsymbol{\theta} + \boldsymbol{\Lambda}\boldsymbol{\rho}(\boldsymbol{\theta}) \tag{5}$$

where $\hat{\mathbf{z}} \in \Re^{n\times 1}$, $\boldsymbol{\rho} \in \Re^{(n\times n_s)\times 1}$; $\quad \boldsymbol{\rho} = \left[\mathbf{r}_1^{\mathrm{T}}\ \mathbf{r}_2^{T}\ ...\ \mathbf{r}_n^{\mathrm{T}}\right]^{\mathrm{T}}$, $\boldsymbol{\alpha} = \left[\beta_{0,1}\ \ \beta_{0,2}\ ...\ \beta_{0,n}\right]^{\mathrm{T}}$,

$$\mathbf{H}(\boldsymbol{\theta}) = \left[H_{ij}\right]_{n\times p} \quad ; \quad H_{ij} = \beta_{j,i} + \theta_j\beta_{jj,i} + \frac{1}{2}\sum_{\substack{k=1\\k\neq j}}^{p}\beta_{kj,i}\theta_k$$

and $\boldsymbol{\Lambda} = \left[\Lambda_{ij}\right]_{n\times(n\times n_s)}$

$$\Lambda_{ij} = \begin{cases} \lambda_{j,i} & (i-1)\,n_s + 1 \le j \le i\times n_s \\ 0. & elsewhere \end{cases}$$

where $\beta_{.,i}$ and $\lambda_{.,i}$ are regression coefficients at the i^{th} output (the calculation of regression coefficients is explained in [11]), $\mathbf{r}_i(\boldsymbol{\theta}) = \left[C_i\left(\boldsymbol{\theta},\boldsymbol{\theta}^{(1)}\right)\ C_i\left(\boldsymbol{\theta},\boldsymbol{\theta}^{(2)}\right)\ ...\ C_i\left(\boldsymbol{\theta},\boldsymbol{\theta}^{(ns)}\right)\right]^{\mathrm{T}}$ and $C_i\left(\boldsymbol{\theta},\boldsymbol{\theta}^{(h)}\right) = \prod_{j=1}^{p} C_{j,i}\left(\theta_j,\theta_j^{(h)}\right)$ is the correlation function. Different types of correlation functions have been introduced in [15] and [16]. The choice of correlation function depends on underlying behavior of the true response. However, this underlying behavior is often not readily apparent, in which case the following correlation function may be used,

$$C_{j,i}\left(\theta_j,\theta_j^{(h)}\right) = \exp\left(-\zeta_{j,i}\left|\theta_j - \theta_j^{(h)}\right|^{\nu_i}\right) \quad 1 \le \nu_i \le 2 \tag{6}$$

where $\zeta_{j,i}$ (the j^{th} term of the vector $\boldsymbol{\zeta}_i$) and ν_i are parameters of the correlation function at the i^{th} output. The calculation of correlation parameters are discussed in [11, 13]. $\nu_i = 1$ gives an Ornstein-Uhlenbeck process which produces continuous paths but not very smooth. The case $\nu_i = 2$ produces infinity differentiable paths. Therefore the parameter ν_i is related to the smoothness of the function in θ_j coordinate. As it is seen in the Eq. (6), the correlation function is 1 when $\theta_j = \theta_j^h$ and its value reduces as the untried point θ_j goes away from the h^{th} design sample θ_j^h.

In the problem of deterministic model updating it is assumed that the measurements of eigenvalues and eigenvector of one structure have been obtained from experiments [1, 2]. The measured data quantities may be assembled into the measurement vector,

$$\mathbf{z}_m = \left[\begin{array}{cccccccccc} \omega_1^2 & \omega_2^2 & . & . & . & \omega_r^2 & \boldsymbol{\phi}_1^{\mathrm{T}} & \boldsymbol{\phi}_2^{\mathrm{T}} & . & . & . & \boldsymbol{\phi}_r^{\mathrm{T}} \end{array}\right]^{\mathrm{T}} \tag{7}$$

which is entirely real when the system is undamped. Assuming that a set of vectors of measured data are available, the vector of mean values of measured data can be readily obtained. Then the problem of deterministic model updating can be applied to identify the deterministic values of updating parameters. If the solution of the updating problem is unique, then the vector of updated parameters can be represented by a point in the parameter space. An initial hypercube around the updated parameters can be constructed as illustrated in Figure 1. Figure 1 shows specifically the procedure for a dynamic system with two input and two output parameters. The Kriging predictor is used as a surrogate for the finite element model to map the space of the initial hypercube of updating parameters to the space of output parameters. If the mapping is good enough to represent the relationship between the input data and output data then this model can be used to correct the dimensions of initial hypercube of updating parameters based on the available measured data.

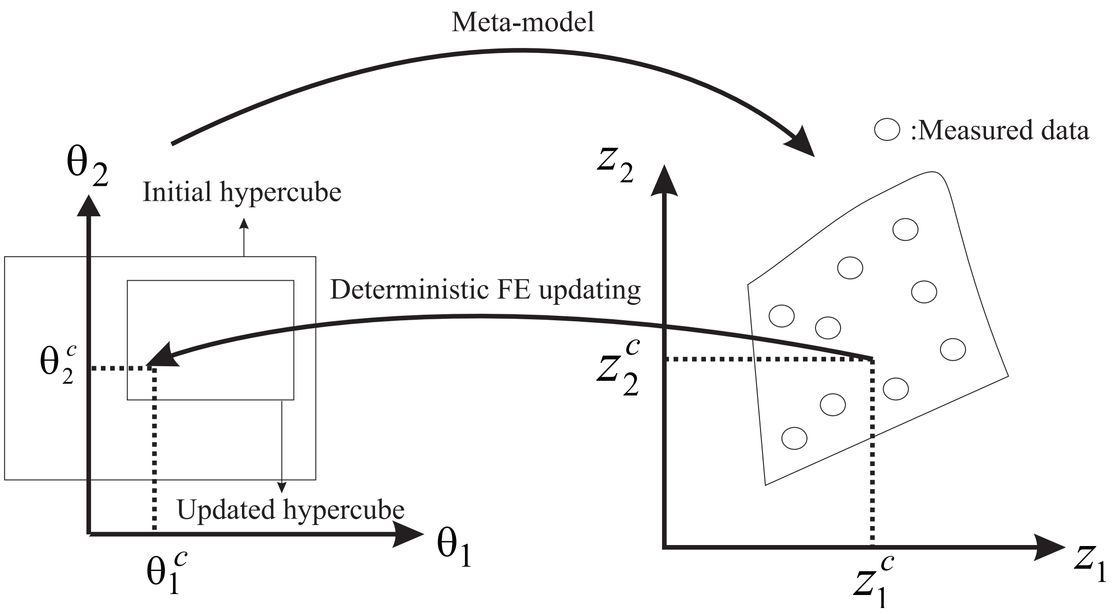

Figure 1: Interval model updating using Kriging model.

Once the initial Kriging model is constructed, the following error function can be defined for deterministic model updating using the Kriging predictor formed from the measured samples,

$$\boldsymbol{\epsilon} = \mathbf{z}_m - (\boldsymbol{\alpha} + \mathbf{H}\boldsymbol{\theta} + \boldsymbol{\Lambda}\boldsymbol{\rho}) = \boldsymbol{\mu} - \mathbf{H}\boldsymbol{\theta} - \boldsymbol{\Lambda}\boldsymbol{\rho} \tag{8}$$

where $\mu = \mathbf{z}_m - \boldsymbol{\alpha}$ and $(\boldsymbol{\theta})$ is omitted from $\mathbf{H}(\boldsymbol{\theta})$ and $\boldsymbol{\rho}(\boldsymbol{\theta})$ for reasons of simplicity. Now the updating problem for each sample of measured data can be stated as an optimisation problem,

$$\min_{\boldsymbol{\theta}} \left(\boldsymbol{\epsilon}^{\mathrm{T}}\boldsymbol{\epsilon}\right) \tag{9}$$

It should be noted that the Kriging model has been constructed and validated for the initial hypercube of the updated parameters. Therefore if the solution of the above minimisation problem converges to a point outside the hypercube, a new Kriging model should be constructed by increasing the size of initial hypercube and the procedure repeated. According to Eq. (8), the error function in Eq. (9) can be expanded as,

$$\begin{aligned}\boldsymbol{\epsilon}^{\mathrm{T}}\boldsymbol{\epsilon} = \boldsymbol{\mu}^{\mathrm{T}}\boldsymbol{\mu} - \boldsymbol{\mu}^{\mathrm{T}}\mathbf{H}\boldsymbol{\theta} - \boldsymbol{\mu}^{\mathrm{T}}\boldsymbol{\Lambda}\boldsymbol{\rho} - \boldsymbol{\theta}^{\mathrm{T}}\mathbf{H}^{\mathrm{T}}\boldsymbol{\mu} + \boldsymbol{\theta}^{\mathrm{T}}\mathbf{H}^{\mathrm{T}}\mathbf{H}\boldsymbol{\theta} \\ + \boldsymbol{\theta}^{\mathrm{T}}\mathbf{H}^{\mathrm{T}}\boldsymbol{\Lambda}\boldsymbol{\rho} - \boldsymbol{\rho}^{\mathrm{T}}\boldsymbol{\Lambda}^{\mathrm{T}}\boldsymbol{\mu} + \boldsymbol{\rho}^{\mathrm{T}}\boldsymbol{\Lambda}^{\mathrm{T}}\mathbf{H}\boldsymbol{\theta} + \boldsymbol{\rho}^{\mathrm{T}}\boldsymbol{\Lambda}^{\mathrm{T}}\boldsymbol{\Lambda}\boldsymbol{\rho}\end{aligned} \tag{10}$$

A necessary condition for minimising the error function Eq. (10) is that,

$$\boldsymbol{\nabla}\left(\boldsymbol{\epsilon}^{\mathrm{T}}\boldsymbol{\epsilon}\right) = \{0\} \quad \boldsymbol{\nabla} = \left\{\frac{\partial}{\partial\theta_j}\right\}_{p\times 1} \tag{11}$$

Substituting Eq. (10) into Eq. (11) leads to,

$$-\mathbf{H}^{\mathrm{T}}\boldsymbol{\mu}-\mathbf{A}\boldsymbol{\theta}-\mathbf{f}\left(\boldsymbol{\theta}\right)+\mathbf{H}^{\mathrm{T}}\mathbf{H}\boldsymbol{\theta}+\mathbf{D}\boldsymbol{\theta}+\mathbf{H}^{\mathrm{T}}\boldsymbol{\Lambda}\boldsymbol{\rho}+\mathbf{V}\boldsymbol{\theta}+\mathbf{U}\boldsymbol{\theta}+\mathbf{g}\left(\boldsymbol{\theta}\right)=\{0\} \tag{12}$$

where $(\boldsymbol{\theta})$ is omitted from $\mathbf{H}(\boldsymbol{\theta})$, $\mathbf{D}(\boldsymbol{\theta})$, $\mathbf{V}(\boldsymbol{\theta})$, $\mathbf{U}(\boldsymbol{\theta})$, $\boldsymbol{\rho}(\boldsymbol{\theta})$ and

$$\mathbf{A}=[A_{ij}]_{p\times p}\,;\quad A_{ij}=\sum_{k=1}^{n}\mu_k\frac{\partial H_{kj}}{\partial\theta_i};\quad \frac{\partial H_{kj}}{\partial\theta_i}=\frac{1}{2}B_{ij,k}$$

$$\mathbf{D}\left(\boldsymbol{\theta}\right)=[D_{ij}]_{p\times p}\,;\quad D_{ij}=\frac{1}{2}\sum_{k=1}^{p}\sum_{l=1}^{n}\left(H_{lj}\frac{\partial H_{lk}}{\partial\theta_i}+H_{lk}\frac{\partial H_{lj}}{\partial\theta_i}\right)\theta_k$$

$$\mathbf{V}\left(\boldsymbol{\theta}\right)=[V_{ij}]_{p\times p}\,;\quad V_{ij}=\sum_{k=1}^{n}\sum_{l=1}^{n_s}\lambda_{l,k}\frac{\partial H_{kj}}{\partial\theta_i}r_{l,k}\left(\boldsymbol{\theta}\right)$$

$$\mathbf{U}\left(\boldsymbol{\theta}\right)=[U_{ij}]_{p\times p}\,;\quad U_{ij}=\sum_{k=1}^{n}\sum_{l=1}^{n_s}\lambda_{l,k}H_{kj}\frac{\partial r_{l,k}\left(\boldsymbol{\theta}\right)}{\partial\theta_i}$$

$$\mathbf{f}\left(\boldsymbol{\theta}\right)=\{f_i\left(\boldsymbol{\theta}\right)\}_{p\times 1}\,;\quad f_i\left(\boldsymbol{\theta}\right)=\sum_{j=1}^{n}\sum_{k=1}^{n_s}\lambda_{k,j}\mu_j\frac{\partial r_{k,j}\left(\boldsymbol{\theta}\right)}{\partial\theta_i}$$

$$\begin{aligned}&\mathbf{g}\left(\boldsymbol{\theta}\right)=\{g_i\left(\boldsymbol{\theta}\right)\}_{p\times 1}\,;\\ &g_i\left(\boldsymbol{\theta}\right)=\frac{1}{2}\sum_{l=1}^{n}\sum_{k=1}^{n_s}\sum_{j=1}^{n_s}\lambda_{j,l}\lambda_{k,l}\left(r_{k,l}\left(\boldsymbol{\theta}\right)\frac{\partial r_{j,l}\left(\boldsymbol{\theta}\right)}{\partial\theta_i}+r_{j,l}\left(\boldsymbol{\theta}\right)\frac{\partial r_{k,l}\left(\boldsymbol{\theta}\right)}{\partial\theta_i}\right)\end{aligned}$$

Eq. (12) can be rearranged for the solution of system parameters $\boldsymbol{\theta}$ as,

$$\left(\mathbf{H}^{\mathrm{T}}\mathbf{H}+\mathbf{D}+\mathbf{U}+\mathbf{V}-\mathbf{A}\right)\boldsymbol{\theta}=\mathbf{f}\left(\boldsymbol{\theta}\right)+\mathbf{H}^{\mathrm{T}}\boldsymbol{\mu}-\mathbf{H}^{\mathrm{T}}\boldsymbol{\Lambda}\boldsymbol{\rho}-\mathbf{g}\left(\boldsymbol{\theta}\right) \tag{13}$$

Since the matrix $\left(\mathbf{H}^{\mathrm{T}}\mathbf{H}+\mathbf{D}+\mathbf{U}+\mathbf{V}-\mathbf{A}\right)$ is a function of $\boldsymbol{\theta}$ an iterative procedure needs to be defined. However, the solution needs the inverse of matrix $\left(\mathbf{H}^{\mathrm{T}}\mathbf{H}+\mathbf{D}+\mathbf{U}+\mathbf{V}-\mathbf{A}\right)$. If this matrix is not invertible an arbitrary weighting matrix can be added to the both sides of Eq. (13) as,

$$\left(\mathbf{H}^{\mathrm{T}}\mathbf{H}+\mathbf{D}+\mathbf{U}+\mathbf{V}-\mathbf{A}+\mathbf{W}\right)\boldsymbol{\theta}=\mathbf{f}\left(\boldsymbol{\theta}\right)+\mathbf{H}^{\mathrm{T}}\boldsymbol{\mu}-\mathbf{H}^{\mathrm{T}}\boldsymbol{\Lambda}\boldsymbol{\rho}-\mathbf{g}\left(\boldsymbol{\theta}\right)+\mathbf{W}\boldsymbol{\theta} \tag{14}$$

and following recursive equation is formed for the solution of Eq. (12),

$$\begin{aligned}\boldsymbol{\theta}_{l+1}=&\left(\mathbf{H}^{\mathrm{T}}\mathbf{H}+\mathbf{D}+\mathbf{U}+\mathbf{V}-\mathbf{A}+\mathbf{W}\right)^{-1}_{|\boldsymbol{\theta}=\boldsymbol{\theta}_l}\\ &\times\left\{\mathbf{f}\left(\boldsymbol{\theta}\right)+\mathbf{H}^{\mathrm{T}}\boldsymbol{\mu}-\mathbf{H}^{\mathrm{T}}\boldsymbol{\Lambda}\boldsymbol{\rho}-\mathbf{g}\left(\boldsymbol{\theta}\right)+\mathbf{W}\boldsymbol{\theta}\right\}_{|\boldsymbol{\theta}=\boldsymbol{\theta}_l}\end{aligned} \tag{15}$$

The iterations continue until convergence on the system parameters $\boldsymbol{\theta}$ is achieved. The matrix $\mathbf{W}$ is chosen so that the matrix $\left(\mathbf{H}^{\mathrm{T}}\mathbf{H}+\mathbf{D}+\mathbf{U}+\mathbf{V}-\mathbf{A}+\mathbf{W}\right)$ is invertible.

The procedure for interval model updating can be defined as follows:

1. Select and update the parameters of the mathematical/FE Model using the mean vector of measured data.

2. Initialize a hypercube around the updated parameters of Finite Element model.

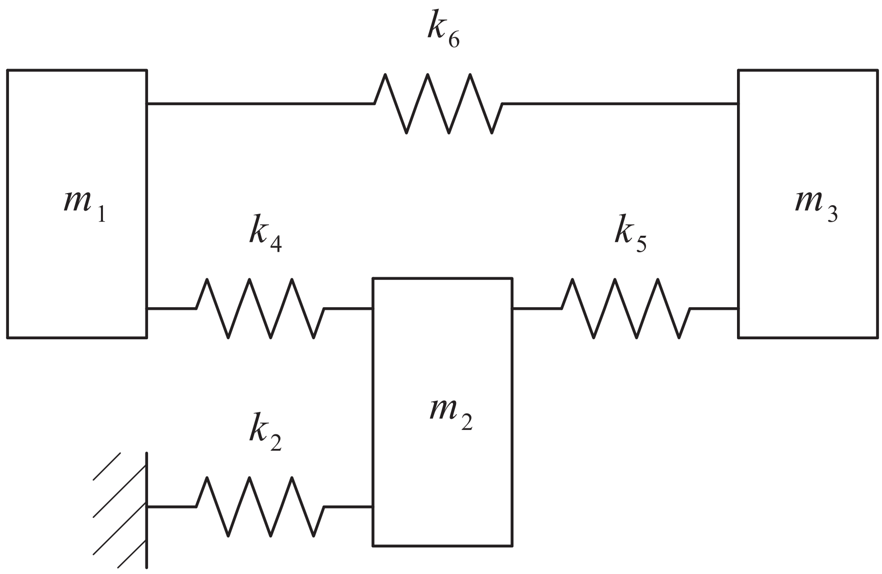

Figure 2: Three degree of freedom system.

3. Construct a meta-model based on updated mathematical/FE Model data. This meta-model should describe the relationship between output data and input data within the initial hypercube around the updated parameters accurately.

4. Use the meta-model for updating the initial hypercube by using all sets of measured data.

5. Construct the new hypercube on the region of updated parameters. If the updated hypercube is bigger than the initial hypercube increase the size of initial hypercube and go back to step 3; otherwise go to step 6.

6. Generate output data by using the meta-model to find the region of variation of output data and compare it with scatter of measured data.

7. End.

3 Numerical Case Study: 3-degree of freedom mass-spring system with close modes

The three degree of freedom mass-spring system, shown in Figure 2 with close modes is considered in this section. The quantification of uncertainty in a dynamic system with close modes is a difficult problem due to non-smoothness of the response surface. Therefore a close mode system is chosen for illustration of the performance of the interval model updating using Kriging method. It is assumed that the true value of the unknown uncertain parameters of the system are given by,

$$k_2 = [7.5 \quad 8.5] \quad \mathrm{kN/m}, \ \ k_4 = [1.8 \quad 2.2] \quad \mathrm{kN/m}, \ \ k_5 = [1.8 \quad 2.2] \quad \mathrm{kN/m}$$

and other parameters are as assumed as $m_1 = 1\,\mathrm{kg}$, $m_2 = 4\,\mathrm{kg}$, $m_3 = 1\,\mathrm{kg}$, $k_6 = 1\,\mathrm{kN/m}$. 10 measured samples are taken for analysis. The initial estimates of the bounds of uncertain parameters are,

$$k_2 = [6.5 \quad 9.5] \quad \mathrm{kN/m}, \ \ k_4 = [1.6 \quad 2.4] \quad \mathrm{kN/m}, \ \ k_5 = [1.6 \quad 2.4] \quad \mathrm{kN/m}$$

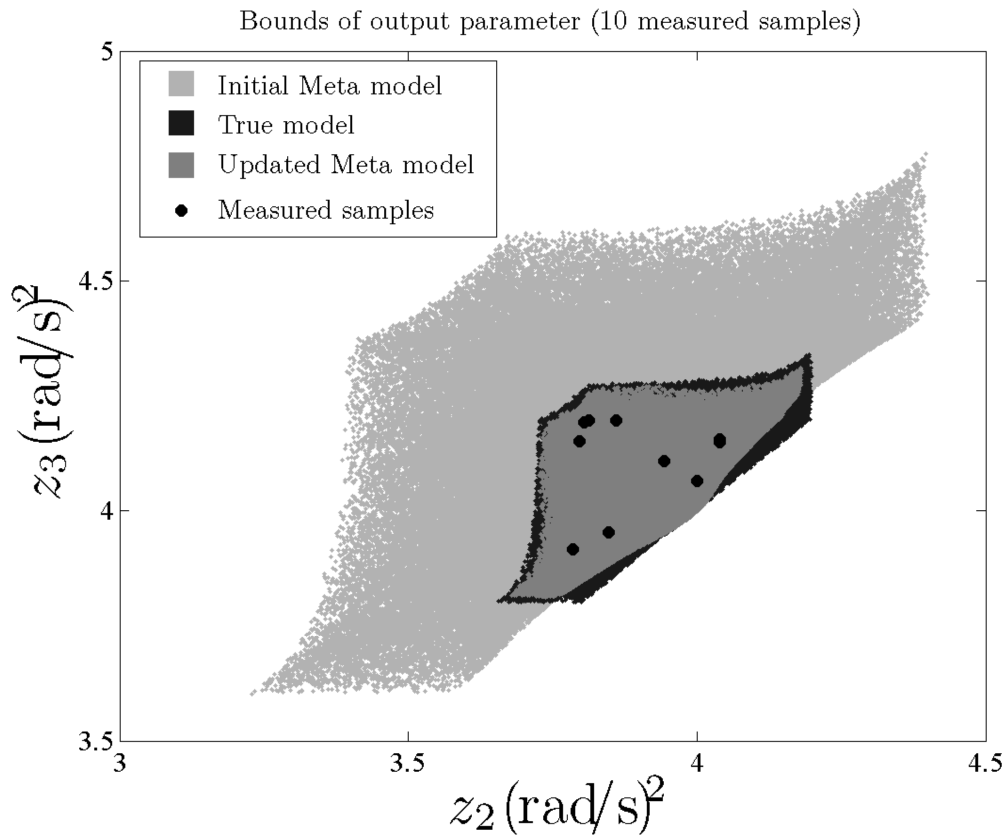

Figure 3: Initial, updated and true spaces of predicted data (100,000 points) based upon 10 measurement samples (system with close modes).

The application of interval model updating is illustrated for correcting the bounds of the updating parameters. The output data are assumed to be the first three eigenvalues and the absolute value of first component of the first eigenvector (ϕ_{11}). The level of confidence of the predictions at untried points can be assessed by evaluating the mean squared error MSE which is discussed in [11, 14]. Fifteen samples were taken from the space of the initial hypercube of updating parameters according to central composite design (CCD). The MSE results show that the initial samples based on CCD with one centre point [17] are not good enough for mapping the initial hypercube of input data to the output data. Therefore the procedure of sampling, described in [11, 14], has been used to improve the Kriging model.

The Kriging model was constructed using a first order polynomial and results obtained using 10 measured samples are shown in Table 1. These results confirm that the modified bounds of uncertain parameters have been determined with very good accuracy. Also, Figure 3 shows that the updated space of the second and third eigenvalues (close modes) obtained by the Kriging model are in good agreement with the true space of the second and third eigenvalues. The latter is obtained by direct solution of the eigenvalue problem of the dynamic system. A good agreement between the updated spaces and the true spaces of other output data are achieved.

It is observed that the evolution of error function, Eq. (10) fails to converge when $(a)\,\mathbf{W} = \mathbf{0}$, due to ill-conditioning. This problem is overcome by using the technique described in Eq. (15). The components of the weighting matrix may be chosen by the analyst and usually depend on the particular problem considered. The weighting matrix $\mathbf{W}$, introduced in Eq. (15), was set to 10 $\mathbf{I}$ (identity matrix) in this case.

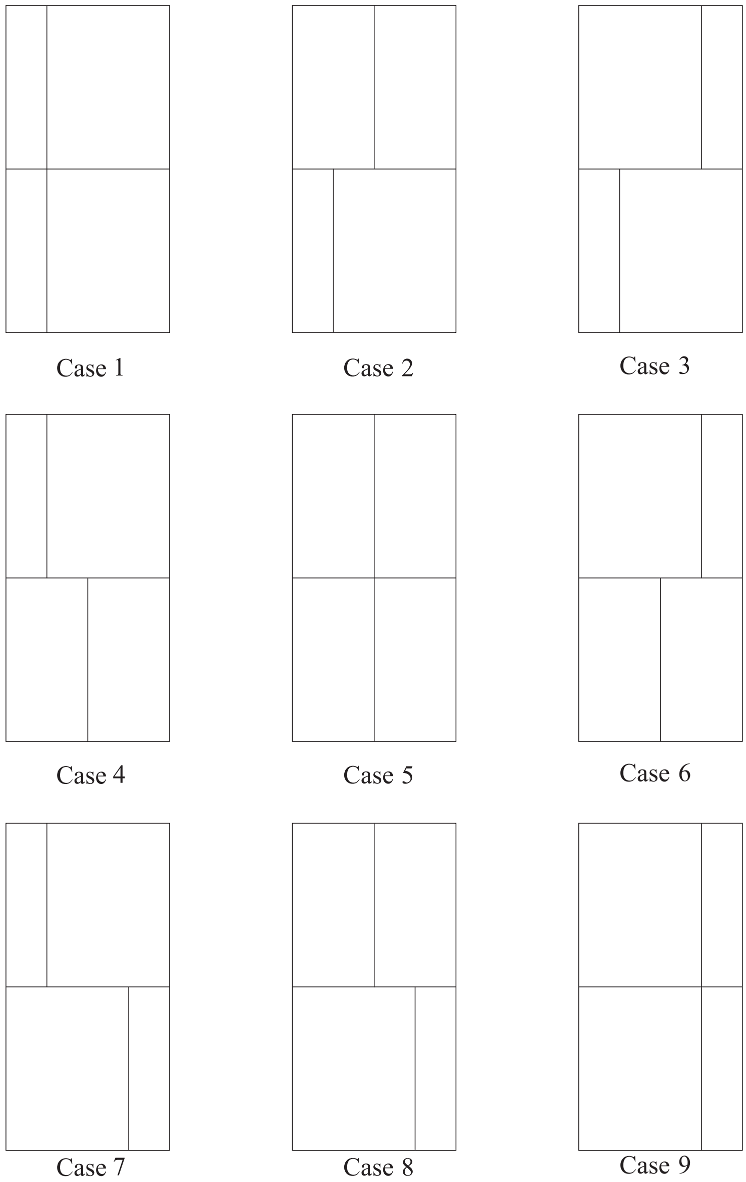

Figure 4: Beam locations in frame structure.

4 Experimental case study: Frame structure with uncertain beams positions

In this section the application of the method to a physical case is studied. The structure is a frame with two internal beams, each of them is designed to be independently located at three different positions. Nine different combinations of beam positions can be provided as shown in Figure 4. All nine cases are modelled in detail using 8-noded solid elements (CHEXA) in MSC-NASTRAN. The physical structure and the finite element model in one configuration of the internal beams are shown in Figure 5(a) and in Figure 5(b) respectively. The bolted joint connections are modelled using rigid elements over an area three times greater than the cross-section of the bolts. The boundary conditions where the frame is connected to a rigid base are represented by fixing the nodal displacements in the three translational degrees of freedom over an area corresponding to the size of a washer between the frame and the base.

The natural frequencies and mode shape of the frame are obtained by doing an instrumented hammer modal test in free-free condition for case 1 and also when fixed to the rigid base for all nine configurations. The experimental results and finite element predictions for frame when fixed to the rigid base for internal beams locations arranged as case 1 is shown in Table 2. The closeness of the finite element predictions to the natural frequencies found in the modal test shows that the frame structure and the boundary conditions are accurately modelled. The finite element predictions and measured data are also found to be in good agreement for free-free boundary conditions and when fixed to the rigid base for cases 2 to 8, reported in [11].

The positions (θ_1 and θ_2) of the two internal beams are assumed to be the unknown updating parameters as indicated in Figure 6 for the purpose of application of interval model updating to this problem. In conventional model updating this choice of updating parameters would require remeshing of the finite element model at each iteration, which is time consuming and inelegant. An important advantage of Kriging interpolation is that the updating of nodal coordinates is as straightforward as any other parameter.

The initial bounds on θ_1 and θ_2 are assumed to be $[0.5\ 2.5]$ and a Kriging model is constructed as a surrogate for the detailed FE model. The relationship between the input parameters (θ_1 and θ_2) and 6 outputs, the first and second in-plane and out-of-plane bending modes and the first and second torsion modes in Tables 2, is described by the Kriging model. The maximum value of the MSE shows that the CCD design together with 9 samples in Figure 4 provide an accurate fit. The locations of internal beams are identified using the optimisation procedure described in Section 2.2.1 based on 6 measured frequencies. As result of identification method the bounds of the updated parameters are corrected. The weighting matrix was set to $W = 100I$ in this case. The initial and identified beams locations in 9 cases obtained by deterministic model updating are shown in Table 3. The maximum error of 11.00 % in Table 3 is an indicator of good performance.

The Kriging model was used to generate all possible variations of the 6 outputs due to the variation of the internal beam locations in the range of [1.00 2.99] for θ_1 and [0.89 3.09] for θ_2. The initial and updated regions of possible natural frequency variation in (a and b) the planes of first and third natural frequencies, (c and d) the planes of second and fifth natural frequencies and (e and f) the planes of fourth and sixth natural frequencies together with 9 measured samples is showed in Figure 7. It is seen from Figures 7(b), 7(d) and 7(f) that the updated regions encloses some measured samples but not all of them. Supposedly the samples are positioned on the boundaries but owing to some errors due to other source of uncertainty (e.g. measurement noise) the samples are found to move slightly over the boundaries. The initial and updated bounds of natural frequencies are shown in Table 4. The maximun error is 4.24% that shows good agreement between the updated model output bounds and the bounds of the measaured data.

5 Conclusion

The problem of interval model updating in the presence of test structure variability is formulated. The parameter vertex solution can be used to solve the problem when the output data are the eigenvalues of the dynamic system and updating parameters are substructure mass and stiffness coefficients. In the general case, the Kriging predictor as a meta-model is used for the solution of interval model updating. A framework for the solution of interval model updating is formulated. The method is verified numerically in a three degree of freedom mass-spring system with close modes. With a very small number of measured samples, the interval model updating was successful in identifying the input parameters with very good accuracy which shows a significant advantage of interval updating over probabilistic methods. The Kriging interpolation was also applied to the frame structure with uncertain positions of internal beams which are treated as updating parameters. The initial erroneous bounds on the beam positions are corrected by using the proposed interval model updating in this paper.

Acknowledgements

This work is funded by the European Union for the Marie Curie Excellence Team ECERTA under contract MEXT-CT-2006 042383.

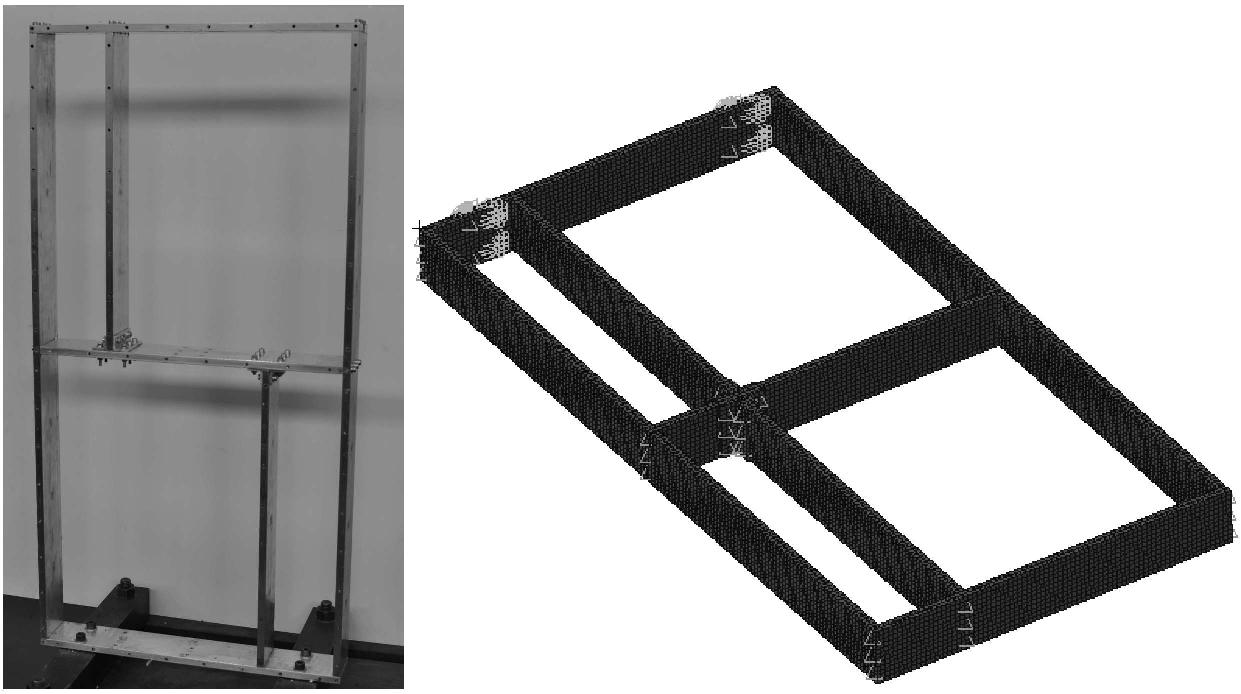

(a) (b)

Figure 5: (a) Frame structure (b) Finite element model.

Table 1: Updated results: 3 DOF mass-spring system with close modes

Parameters	Initial error %	Updated error % 10 Measured samples
k_1	$[-13.3 \quad 11.8]$	$[0.6 \quad -0.7]$
k_2	$[-11.1 \quad 9.1]$	$[0.8 \quad -1.0]$
k_5	$[-11.1 \quad 9.1]$	$[0.4 \quad -0.5]$

Table 2: Measured and FE predictions of natural frequencies -case 1

	Measured (Hz)	FE (Hz)	FE error %	Mode shape
Mode (1)	22.54	22.59	0.22	**first in-plane bending mode**
Mode (2)	27.84	27.27	-2.04	**first out-of-plane bending mode**
Mode (3)	47.63	48.14	1.08	**first torsion mode**
Mode (4)	81.19	80.89	-0.37	**second in-plane bending mode**
Mode (5)	201.35	201.55	0.10	higher order in-plane bending mode
Mode (6)	233.71	233.41	-0.13	higher order in-plane bending mode
Mode (7)	256.40	259.05	1.03	**second out-of-plane bending mode**
Mode (8)	257.68	256.54	-0.44	higher order in-plane bending mode
Mode (9)	283.09	283.35	0.09	higher order in-plane bending mode
Mode (10)	298.46	305.34	2.30	higher order in-plane bending mode
Mode (11)	312.39	316.49	1.31	**second torsion mode**

References

[1] J.E. Mottershead, M.I. Friswell, *Model updating in structural dynamics: a survey*, Journal of Sound and Vibration, Vol. 167, No. 2 (1993), pp. 609-625.

[2] M.I. Friswell, J.E. Mottershead, *Finite Element Model Updating in Structural Dynamics*, Kluwer Academic Press (1995), Dordrecht.

[3] J.D. Collins, G.C. Hart, T.K. Hasselman, B. Kennedy, *Statistical identification of structures*, AIAA Journal, Vol. 12, No. 2 (1974), pp. 185-190.

[4] M.I. Friswell, *The adjustment of structural parameters using a minimum variance estimator*, Mechanical Systems and Signal Processing, Vol. 3, No. 2 (1989), pp. 143-155.

[5] J.R. Fonseca, M.I. Friswell, J.E. Mottershead, A.W. Lees, *Uncertainty identification by the maximum likelihood method*, Journal of Sound and Vibration, Vol. 288, No. 3 (2005), pp. 587-599.

[6] X.G. Hua, Y.Q. Ni, Z.Q. Chen, J.M. Ko, *An improved perturbation method for stochastic finite element model updating*, International Journal for Numerical Methods in Engineering, Vol. 73, No. 13 (2008), pp. 1845-1864.

[7] H. Haddad Khodaparast, J.E. Mottershead, M.I. Friswell, *Perturbation methods for the estimation of parameter variability in stochastic model updating*, Mechanical Systems and Signal Processing, Vol. 22, No. 8 (2008), pp. 1751-1773.

[8] H. Haddad Khodaparast, J.E. Mottershead, *Efficient Methods in Stochastic Model Updating*, in *Proceedings of International Conference on Noise and Vibration, ISMA2008, 2008 September 27-30*, Leuven, Belgium (2008), pp. 1855-1869.

[9] Y. Govers, M. Link, *Stochastic model updating: Covariance matrix adjustment from uncertain experimental modal data*, Mechanical Systems and Signal Processing, Vol. 24, No. 3 (2010), pp. 696-706.

[10] Z. Qui, X. Wang, M.I. Friswell, *Eigenvalue bounds of structures with uncertain-but-bounded parameters*, Journal of Sound and Vibration, Vol. 282, No. 1-2 (2005), pp. 297-312.

[11] H. Haddad Khodaparast, J.E. Mottershead, K.J. Badcock, *Interval model updating in structural dynamics*, Mechanical Systems and Signal Processing, submitted (2010).

[12] R. Fox and M. Kapoor, *Rates of change of Eigenvalues and Eigenvectors*, AIAA Journal, Vol. 6, No. 12 (1968), pp. 2426-2429.

[13] J. Sacks, W.J. Welch, T.J. Mitchell, H.P. Wynn, *Design and Analysis of Computer Experiments*, Statistical Science, Vol. 4, No. 4 (1989), pp. 409-435.

[14] M. Ghoreyshi, K.J. Badcock, M.A. Woodgate, *Accelerating the Numerical Generation of Aerodynamic Models for Flight Simulation*, Journal of Aircraft, Vol. 46, No. 3 (2009), pp. 972-980.

[15] E.H. Isaaks, R.M. Srivastava, *An Introduction to Applied Geostatistics*, Oxford University Press, (1989), New York, USA.

[16] S.N Lophaven, H.B Nielsen, J. Sndergaard, *DACE, A MATLAB Kriging Toolbox*, Technical Report I, Technical University of Denmark, (2002), MM-TR-2002-12, DK-2800 Kgs. Lyngby Denmark.

[17] R.H. Myers, D.C. Montgomery, *Response surface methodology; process and product optimisation using designed experiments*, John Wiley and Sons, (2002), New York, USA.

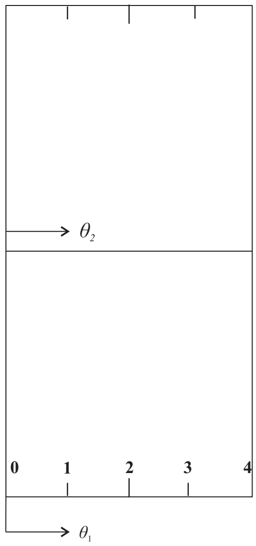

Figure 6: Parametrisation of internal beam locations in frame structure.

Table 3: Deterministic model updating of beam locations

True parameters		Initial parameters		Updated parameters		Initial error %		Updated error %	
θ_1	θ_2	θ_1	θ_2	θ_1	θ_2	θ_1	θ_2	θ_1	θ_2
1.0	1.0	1.6	1.6	1.04	1.02	60.00	60.00	3.73	2.00
1.0	2.0	1.6	2.4	1.00	2.15	60.00	20.00	-0.21	7.56
1.0	3.0	1.6	2.4	1.00	3.08	60.00	-20.00	0.20	2.76
2.0	1.0	1.6	1.6	2.04	0.90	-20.00	60.00	1.81	-9.78
2.0	2.0	2.4	2.4	2.13	2.00	20.00	20.00	6.48	-0.12
2.0	3.0	2.4	2.4	1.95	3.09	20.00	-20.00	-2.36	3.06
3.0	1.0	2.4	1.6	2.98	0.89	-20.00	60.00	-0.58	-11.00
3.0	2.0	2.4	1.6	2.99	1.83	-20.00	-20.00	-0.31	-8.36
3.0	3.0	2.4	2.4	2.93	2.98	-20.00	-20.00	-2.18	-0.58

Table 4: Measured, initial and updated bounds of natural frequencies (fixed-frame structure)

	Measured (Hz)	Initial FE (Hz)	Updated FE (Hz)	Initial FE % error	Updated FE % error
First in-plane bending mode	$[22.54\ \ 24.34]$	$[21.62\ \ 24.61]$	$[22.57\ \ 24.61]$	$[-4.08\ \ 1.11]$	$[0.13\ \ 1.11]$
First out-of-plane bending mode	$[24.38\ \ 27.84]$	$[23.66\ \ 35.53]$	$[23.86\ \ 27.47]$	$[-2.95\ \ 27.62]$	$[-2.13\ \ -1.33]$
First torsion mode	$[47.13\ \ 49.85]$	$[43.72\ \ 67.57]$	$[45.13\ \ 50.55]$	$[-7.24\ \ 35.55]$	$[-4.24\ \ 1.40]$
Second in-plane bending mode	$[74.38\ \ 81.19]$	$[71.09\ \ 82.50]$	$[73.99\ \ 81.37]$	$[-4.42\ \ 1.61]$	$[-0.52\ \ 0.22]$
Second out-of-plane bending mode	$[219.48\ \ 256.40]$	$[224.08\ \ 267.34]$	$[224.08\ \ 259.51]$	$[2.10\ \ 4.27]$	$[2.10\ \ 1.21]$
Second torsion mode	$[299.72\ \ 312.39]$	$[300.26\ \ 339.65]$	$[303.58\ \ 317.20]$	$[0.18\ \ 8.73]$	$[1.29\ \ 1.54]$

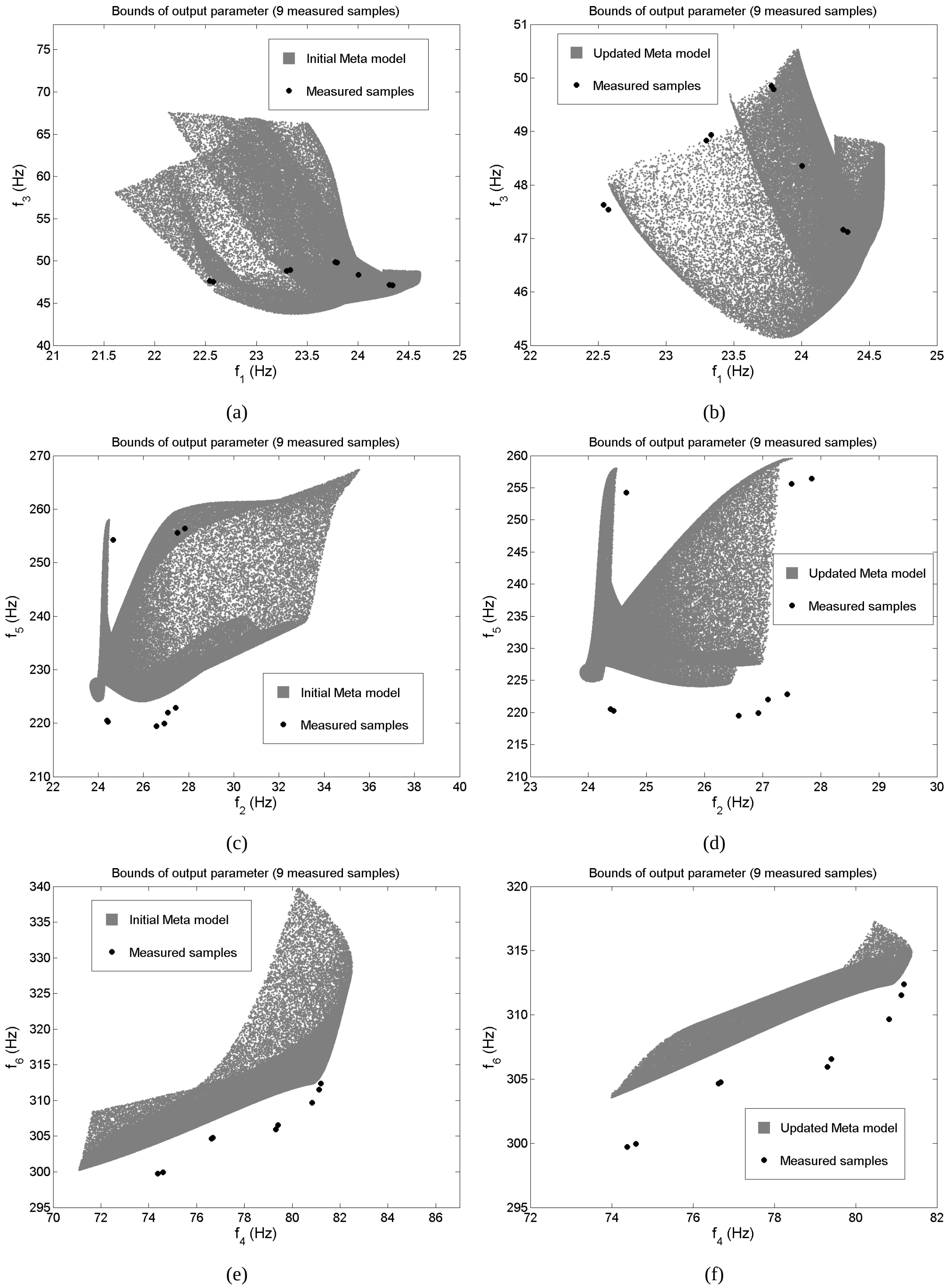

Figure 7: Initial and updated spaces of predicted data (100,000 points) based upon 9 measurement samples (frame structure)